PANAMGEO CHILE 2024
17th PAN-AMERICAN CONFERENCE ON SOIL MECHANICS AND GEOTECHNICAL ENGINEERING | 2nd LATIN-AMERICAN REGIONAL CONFERENCE OF IAEG
LA SERENA • CHILE / NOVEMBER 12 - 16, 2024

Proceedings of the 17th Pan-American Conference on Soil Mechanics and Geotechnical Engineering (XVII PCSMGE), and 2nd Latin-American Regional Conference of the International Association for Engineering Geology and the Environment (IAEG), La Serena Chile, 2024.

Use of Multi-Temporal UAV Imagery for Machine Learning Based Estimation of Soil Moisture and Vegetation Greenness

Uso de imágenes UAV multitemporales para la estimación basada en aprendizaje automático de la humedad del suelo y el verdor de la vegetación

Dr. Daniel Francis & Dr. Sebastian Bryson
Civil Engineering, University of Kentucky, United States of America, danny.francis@uky.edu (Same affiliation)

Batmyagmar Dashbold
Geotechnical Engineering, Stantec Inc., United States of America

ABSTRACT: Herein, we present a workflow through which a small unmanned aerial vehicle (UAV), equipped with an optical digital camera, was used to extract soil and vegetation parameters. Multi-temporal digital images were acquired across a three-month period over a site previously observed to be susceptible to landslide occurrence. After acquisition, the images were ortho-rectified using matching points by analyzing all images employing scale invariant feature transform (SIFT) and bundle block adjustment techniques. Once ortho-rectified, the images were co-registered employing fully automatic tie point generation through an area-based matching technique. After processing, the images were deconstructed into respective Red, Green, and Blue (RGB) light bands. Statistics were then computed for each RGB band and used to develop a feature set for a linear regressive machine learning approach. As in-situ measurements were not available, soil moisture and vegetation greenness estimates were obtained via the GLDAS and NASA SMAP missions and substituted. Efforts herein yielded a workflow capable of predicting soil moisture at root zone (0-100 cm) (R^2=0.65), soil moisture at depth (100-200 cm) (R^2=0.57), and vegetation greenness (R^2=0.89) as a function of RGB imagery.

KEYWORDS: Landslides, UAV, Soil Moisture, Machine Learning, Multi-Temporal

1 INTRODUCTION

Many researchers have shown soil moisture to be a contributing factor in both slope stability and the triggering of landslides (Hong et al., 2007; Zhuo et al., 2019; Wicki et al., 2020). Landslides are very common dangerous natural hazards that occur worldwide. The occurrence of these hazards is often accompanied by damage to public and private properties as well as losses of life. (Klose et al. 2014). Mapping and monitoring of slopes that are susceptible to landslide occurrence is a crucial issue for potential prevention and assessment of these hazards (Rossi et al. 2018). Many different approaches exist for mapping and monitoring these susceptible areas. Typically, rainfall thresholds are used as a means to indicate a potential triggering of a landslide through either hazard assessments or early warning systems (Crozier 1997; Segoni et al. 2018). However, in many cases, early warnings based solely on rainfall are not adequate because antecedent soil moisture conditions (i.e., soil moisture conditions *prior* to rainfall) play a crucial role in the initiation of landslides (Zhuo et al. 2019). Therefore, a means to actively monitor soil moisture over landslide susceptible areas is desired.

A simple means to monitor soil moisture over desired areas would be through installation of monitoring devices. However, this installation would likely be costly and only effective for the given site of installation. Herein, an Unmanned Aerial Vehicle (UAV) was used as a means to monitor soil moisture and vegetation greenness, due to its responses to soil moisture (Ugbaje et al., 2020), using aerial imagery. Past researchers have implemented the use of machine learning techniques to extract soil moisture from imagery (Ge et al. 2019; Lu et al., 2020). However, these past efforts focused upon implementation of hyperspectral images (i.e., images that account for wide spectrums of light). Alternatively, this study investigates simple digital imagery, in conjunction with machine learning, as a means to obtain desired parameters. Unlike hyperspectral imagery, digital imagery is composed of only three light bands: Red, Green, and Blue (i.e., RGB). As digital imaging sources are widely available, utilization of digital imaging greatly simplifies the process of monitoring parameters over desired areas.

As with hyperspectral imaging, past research has been conducted to investigate digital imagery as a means to measure soil moisture (Dos Santos et al., 2014; Zanetti et al., 2015). However, past research implemented either extensive machine learning approaches (neural networks) or prepared lab-based samples of soil for imaging. This study presents a novel approach for direct acquisition of physical parameters from digital imagery. Efforts are made to: (1) Obtain UAV-based digital imagery of in-situ conditions over an area observed to be previously susceptible to landslide occurrence and (2) Investigate a more simplistic linear regressive machine learning approach to acquire desired parameters from digital imagery. To do so, a UAV with an optical digital camera was used to capture 20 multi-temporal RGB images spanning a three-month period over an area where a landslide occurred in the past. The UAV images were post-processed to be ortho-rectified and co-registered through algorithms available in the PIX4D photogrammetric software (https://www.pix4d.com). Once post-processed, the images were deconstructed into respective Red, Green, and Blue bands.

Statistics were then computed for each RGB band to develop a feature set for associated regressive machine learning. As no in-situ data was readily available, estimates from the Global Land Data Assimilation System (GLDAS) and NASA Soil Moisture Active Passive (SMAP) Earth-Observing satellite mission were substituted. This work develops a workflow through which digital imagery can be obtained and effectively utilized to estimate soil moisture and vegetation greenness over a given study area.

2 STUDY AREA

A landslide, documented by the Kentucky Geological Survey (https://www.uky.edu/KGS/), was chosen as the study area. This known landslide occurred on 7/7/1995 at a latitude and longitude of 37.709° and -84.503°, respectively, in Garrard County, Kentucky. The KGS report for this slide indicates the cause was that of a heavy rainfall event. Therefore, it is assumed that soil moisture has historically led to landslide occurrence at this site. As this study focuses upon soil moisture as an indicator of slope stability, such a site becomes a prime area of study. The location of the studied landslide within Garrard County is shown in Figure 1.

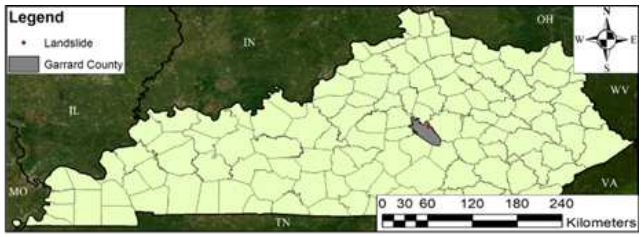

Figure 1. Studied 1995 Landslide Located in Garrard County, Kentucky

3 UAV SPECIFICATIONS AND OPERATION

The UAV used was that of a DJI Phantom 4 Advanced Quadcopter. This UAV is equipped with a high resolution 20-megapixel camera that offers exceptional image quality. Additionally, this UAV is able to both autonomously fly and capture imagery along a predefined flight path. This autonomous operation, in conjunction with consistent camera parameters, allows imagery to remain consistent across current and subsequent flights. Consistent imagery is necessary for proper image processing conducted over the study area. Autonomous flight of the UAV was conducted through implementation of PIX4Dcapture. PIX4Dcapture is a flight planning and image acquisition app developed for Android and iOS mobile operating systems by Pix4D.

Pix4D was used to establish the flight path and altitude parameters for the UAV. The flight altitude was established at 62 m. This altitude was observed to provide sub-meter spatial resolution of the aerial imagery for desired quality. Additionally, Pix4D was used to establish overlapping of acquired aerial imagery. The forward and side overlap for the autonomous flight are highly critical for successfully constructing RGB orthoimages or reflectance maps (Guan et al. 2019). The flight path was constructed such that an 80 percent frontal and 60 percent lateral overlap were established. With the altitude and overlapping parameters established, the spatial area and resolution of each image was roughly 4428 m^2 and 0.05 m/pixel, respectively. As discussed, 20 of these autonomous flights were conducted over the study area over a 3-month span. These flights were conducted between 1100 and 1600 (Eastern Time, USA) on days with less than 20 percent cloud coverage in an attempt to keep the lighting consistent across the imagery. Figure 2 shows the studied landslide area, with extents of the 1995 slide indicated, as well as the implemented flight path over said area.

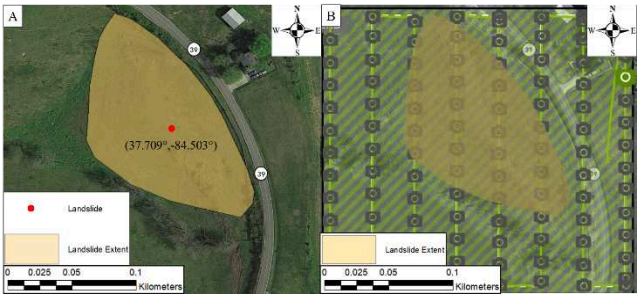

Figure 2. (A) 1995 Landslide Extents at Study Site in Garrard County, Kentucky and (B) Aerial View of UAV Flight Path (camera logo indicates location UAV will stop and take an aerial image)

4 POST-FLIGHT IMAGE PROCESSING

Imagery acquired via the various UAV flights required post-flight processing before assimilation into soil parameter extraction analyses. This post-processing ensures that each pixel within the imagery corresponds to the correct ground position.
Post-processing was conducted through photogrammetric orthorectification. Orthorectification is a process that applies corrections for optical distortions from the sensor system and apparent changes in the position of ground objects caused by the perspective of the sensor view angle and ground terrain (Brown, 2016). After orthorectification, images become precisely registered to a ground coordinate system and experience a constant scale (i.e., no distortions) across the entire image. The orthorectification workflow employs structure from motion (SfM) and multi-view stereopsis (MVS) techniques to construct digital surface models and produce ortho-rectified images. All post-flight image processing was done in the Pix4D mapper photogrammetric software (https://www.pix4d.com/). Pix4D mapper searches for matching points by analyzing all images using the scale invariant feature transform (SIFT) (Lowe 2004) feature matching technique. Additionally, SIFT implements an improved version of binary descriptors proposed in Strecha et al. (2011) to match image and ground-based points quickly and accurately. These matched points, in conjunction with approximate values of image position and orientation, are then used in a bundle block adjustment (Triggs,1999) to reconstruct the exact position and orientation of the camera for every acquired image. Based on this reconstruction, the matching points were verified. Once verified, the 3D coordinates of each point were calculated using GPS measurements from the UAV during flight. These 3D coordinates were then interpolated to form a

triangulated irregular network. This network yielded a digital elevation model (DEM) to project all image pixels and to calculate the geo-referenced ortho-rectified images (Strecha et al. 2012).

In addition to orthorectification, image co-registration was also conducted. Image co-registration is a process through which two or more images are geometrically aligned to fuse corresponding pixels that represent the same object. Typically, the geometric relationship between images is obtained through a number of tie points (a known point present in multiple images). These known points are typically predetermined ground control points (GCPs). However, GCPs were not available for use over the study area. Alternatively, automatic tie point generation can be conducted through an area-based matching technique. This technique compares the gray scale values of two or more images and tries to find conjugate image locations based on similarity of gray scale value patterns. Effectively, if matching gray scale patterns are observed, then it is assumed that a point is present across multiple images and becomes a tie point. The results of area-based matching largely depend upon the quality of the approximate relationship between the images. This is determined through traditional or pseudo rational polynomial coefficients (RPC) map information, or by ensuring three or more tie points exist across the images. Automatic co-registration process was carried out using the ENVI 5.5 (https://www.l3harrisgeospatial.com/) remote sensing software. Figure 3 shows the co-registration of two images using an automatic registration tool. Once the multi-temporal images were orthorectified and co-registered, they were analyzed further to extract soil moisture using a machine learning model.

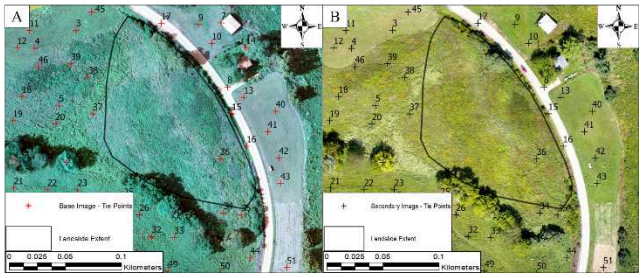

Figure 3. Co-Registration of Images Performed Using ENVI Area Based Matching Technique with Tie Points from: (A) Base Image (8/11/2020) and (B) Secondary Image (9/11/2020)

5 LINEAR REGRESSION EXTRACTION OF PARAMETERS FROM OPTICAL IMAGERY

Multi-temporal ortho-rectified and co-registered images, in conjunction with linear regression, were investigated as a readily available means to extract moisture parameters observed to have an effect on the stability of a given slope. The first parameter extracted was that of soil moisture at various depths (ranging from 0-200 cm). As stated, no in-situ soil moisture measurements were readily available. Therefore, soil moisture estimates from the GLDAS and NASA SMAP Earth-Observing satellite mission were substituted. The spatial resolution of these products is roughly 28 km and 9 km, respectively. Both products have 3-hour temporal resolutions. An additional parameter that was investigated was that of vegetative greenness. Changes in soil moisture are typically quickly reflected by levels of vegetative greenness (Ugbaje and Bishop, 2020), implying that greenness can be investigated as a pseudo indicator of underlying soil moisture. Measurements of greenness were also obtained via the NASA SMAP satellite mission.

Linear regression-based machine learning analyses were conducted to investigate the assumed correlation between discussed parameters and aerial imagery light levels. The imagery used consists of Red, Green, and Blue (RGB) band light levels. When combined, these RGB values yield a true color image (i.e., an image with colors from across the spectrum). The wavelengths, in nanometers, of spectral RGB bands range between 635-700 nm (red), 520-560 nm (green), and 450-490 nm (blue). For use in digital imagery, the brightness values of the RGB bands are scaled to an 8-bit value that ranges between 0 and 255 and become representative of surface reflectance. In this range, a values near or of 0 indicate very low light levels, while a value of 255 indicates high levels of the respective RGB band. Additionally, digital imagery can be deconstructed to yield a pure red light, green light, and blue light image. An example of this deconstruction can be seen in Figure 4, which shows the true color aerial image from 9/9/2020 as well as the respective RGB band light levels across this image.

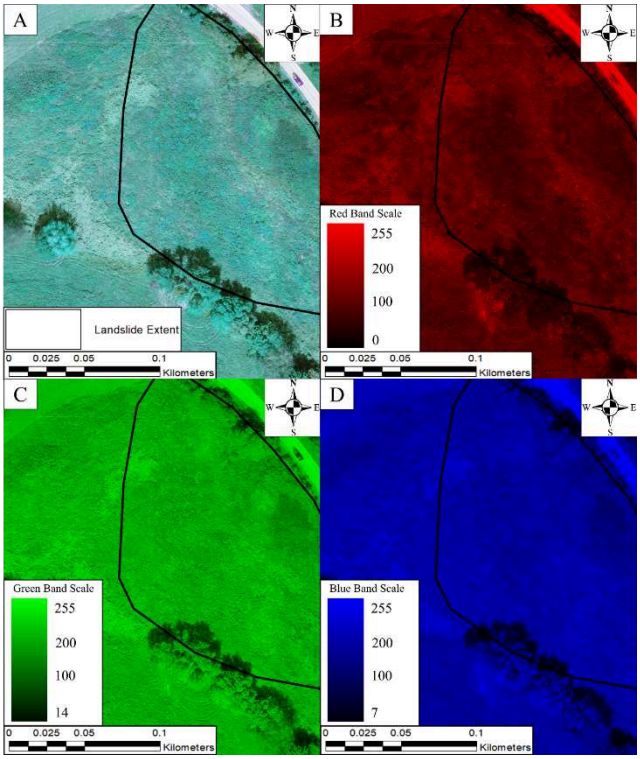

Figure 4. (A) True Color Image from 9/9/2020, (B) Red Band Reflectance, (C) Green Band Reflectance, and (D) Blue Band Reflectance

The deconstruction of aerial imagery into respective RGB bands, as shown in Figure 4, was the first step in the soil parameter

correlation process herein. A linear regression machine learning model was then used to correlate the RGB reflectance values to the GLDAS/SMAP based retrievals of soil moisture and vegetation greenness.

5.1 *Statistical Analyses of RGB Data*

RGB values from aerial imagery were used in an effort to obtain soil moisture parameters from 20 UAV flights. However, these RGB values were not the only implemented dataset for the machine learning process. Alizamir et al. (2020) successfully used a machine learning model with various statistical combinations of variables to predict soil temperature at different depths. Based on this success, various statistical information from the constructed RGB dataset was acquired and implemented to further the performance of machine learning efforts. The statistical values are that of the mean, standard deviation (std), covariance, and eigenvalue. The mean and std were calculated based on individual bands (e.g., mean, and standard deviation of red band). Covariance was calculated between pairs of bands (e.g., Red/Blue, Red/Green, etc.). The covariances were then used to calculate eigenvalues. An eigenvalue decomposition of the covariance matrix can reveal principal directions of variation between images in the collection. This has applications in image coding, image classification, and object recognition. Implementation of these statistical values yielded 12 features for use in later machine learning attempts. These features, as shown in Figure 5, are the three statistics per RGB band (mean, standard deviation, and eigenvalue), and three covariances between bands. All statistics were calculated using the ENVI 5.5 software at a spatial resolution of 15 m over the study area.

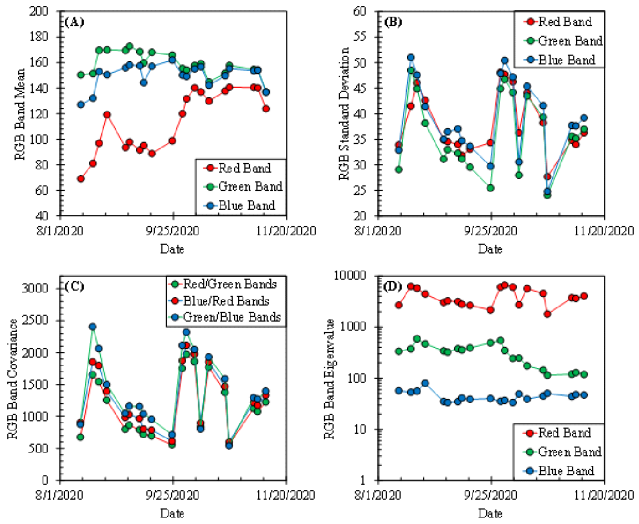

Figure 5. RGB Statistical Data from 20 UAV flights Used as Feature Set for Regressive Machine Learning including (A) Means, (B) Standard Deviations, (C) Band Covariances, and (D) Eigenvalues

5.2 *Linear Regression Prediction of Soil Parameters*

Linear regression is a method used to estimate a target value based on observed predictor values. Herein, the target value is either soil moisture at a given depth or vegetation greenness. Predictor values are those of the 12 features (RGB-based statistical values) discussed previously. Linear regression modelling assumes the target value (soil moisture/greenness) to be a linear combination of the predictor features (RGB statistical values). A generalized approach to linear regression modelling is as follows:

$$\bar{y}(w,x) = w_0 + w_1x_1 + \ldots + w_ix_i \quad (1)$$

where, $\bar{y}$ = target value (moisture or greenness); w_0 = constant intercept; $w_i(i = 1, 2, 3, \ldots, n)$ = coefficient estimates of the model; $x_i(i = 1, 2, 3, \ldots, n)$ = predictor variables (e.g., RGB and statistical values). The coefficients (w_i) express the effects of the predictor variables on the target variable value. Additionally, in an effort to optimize the linear regression-based predictions, gradient descent was implemented. Gradient descent has been observed to effectively improve predictions obtained through linear regressive approaches (Ruder, 2016) and led to observed success in model performance and validation.

5.3 *Model Performance and Validation*

Development of the linear regressive model was conducted using a 75-25 train-test split fashion. In machine learning, this implies that 75 percent of the data being used to build the model is set aside to train the model, while 25 percent of the data is kept from the model during training and is used to gauge model performance after model training is completed. As only 20 UAV flights were conducted over the study area, this implies that only 20 points of data (RGB statistical data) were available for model development. With the established train-test split, 15 points were used to train the model, while 5 points were withheld to gauge performance. The linear regression equations obtained for the investigated parameters are as follows:

$$SMAP_{100} = 82.44 - 0.002x_1 + 133.17x_2 - 723.2x_3 + 402.1x_4 - 204x_5 \quad (2)$$

$$GLDAS_{200} = 297.17 - 26.47x_1 - 360.98x_2 + 2445.5x_3 - 226.9x_4 - 55 \quad (3)$$

$$SMAP_{VG} = 0.93 - 0.06x_1 + 0.087x_2 + 0.659x_3 + 0.057x_4 - 0.424x_5 + \quad (4)$$

where, $SMAP_{100}$ = soil moisture at 100 cm from SMAP; $GLDAS_{200}$ = soil moisture at 200 cm from GLDAS; $SMAP_{VG}$ = vegetation greenness from SMAP; x_1,x_2,x_3 = red band mean, std, and eigenvalue; x_4 = red band/green band covariance; x_5 = red band/blue band covariance; x_6,x_7,x_8 = green band mean, std, and eigenvalue;x_9 = green band/blue band covariance, and x_{10},x_{11},x_{12} = blue band mean, std, and eigenvalue. The results of these machine learning efforts are shown in Figure 6, where "Test Dataset" refers to model predicted values.

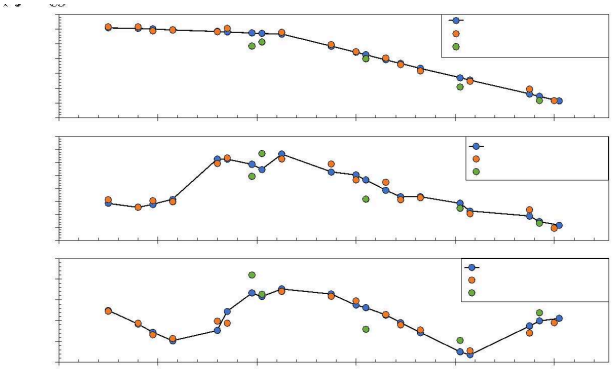

Figure 6. Predicted Target Values Obtained via Linear Regressive Machine Learning Model Compared Against Observed Values via: (A) SMAP Vegetation Greenness, (B) SMAP 100 cm Moisture (%), and (C) GLDAS 200 cm Moisture (kg/m^2)

The performance of these regressive equations was evaluated through use of R^2 values between model predicted and known test points. The R^2 values achieved are as follows: $SMAP_{100}$: 0.65, $GLDAS_{200}$: 0.57, and $SMAP_{VG}$: 0.89. As observed from these metrics, linear regressive machine learning performed strongly in prediction of vegetation greenness. It was expected that the coupling of RGB values derived from vegetation imagery with SMAP-based vegetation greenness estimates would yield a well performing model, as seen herein. As the predictive efforts move deeper into the soil layer, a decrease in the performance of predictive ability is observed. The lowest performance was observed to occur when predicting the deepest-seated parameter (soil moisture at 200 cm), with an R^2 of 0.57. However, the strong performance of the predictive model in estimation of vegetation greenness, a value that reacts to changes in soil moisture (Ugbaje and Bishop, 2020), yields confidence in future abilities of soil moisture prediction.

6 CONCLUSIONS

Herein, a workflow was developed that saw the derivation of soil moisture and vegetation greenness from UAV-based digital aerial imagery. As soil moisture is a predominant controlling factor in landslide occurrence (Hong et al., 2007), the investigation focused on an area previously observed to be susceptible to landslide occurrence. Multiple UAV flights were conducted over the study area with aerial imagery acquired during each flight. Post-processing of the imagery was conducted to both orthorectify and co-register the images. This post-processing ensured that points within imagery corresponded to correct points observed on the ground. Once post-processing was completed, the aerial imagery was deconstructed into respective RGB bands. Statistical analyses were then conducted on the RGB data to obtain the mean, standard deviation, covariance, and eigenvalue for each band. The results of these statistical analyses then became the features of a linear regressive machine learning predictive model. This model was used to estimate desired parameters as a function of the RGB statistical data. However, no in-situ measurements were readily available over the study area for use in the development of this model. To remedy this lack of data availability, GLDAS and NASA SMAP soil moisture estimates and SMAP vegetation greenness estimates were obtained and substituted. With all required data available, the work moved to prediction of the desired parameters over the investigated area. It was observed that linear regressive predictions performed strongly in prediction of vegetation greenness values and adequately in prediction of soil moisture values. However, it is known that vegetation greenness responds somewhat rapidly to changes in underlying soil moisture levels (Ugbaje and Bishop, 2020). This implies that vegetation greenness potentially serves as a viable pseudo indicator of soil moisture levels. It is also thought that the predictive model would benefit from a more robust dataset. Herein, imagery from 20 UAV flights was used to obtain the RGB features for model development. Obtaining more imagery over the study area would yield a more robust dataset and likely lead to observable improvements in predictive abilities. Regardless, this study provides a viable workflow to estimate vegetation greenness and soil moisture values derived solely from UAV-based digital imagery.

7 REFERENCES

Alizamir, M., Kisi, O., Ahmed, A.N., Mert, C., Fai, C.M., Kim, S., Kim, N.W. and El-Shafie, A. (2020). Advanced machine learning model for better prediction accuracy of soil temperature at different depths. *Plos one*, *15*(4), p.e0231055.

Brown, C. (2016). "Defining Imagery." *The arcgis® Imagery book: New view, new vision*, essay, Esri Press, Redlands, CA, 41–42.

Dos Santos, J.F., Silva, H.R., Pinto, F.A. and Assis, I.R.D. (2016). Use of digital images to estimate soil moisture. Revista Brasileira de Engenharia Agrícola e Ambiental, 20(12), pp.1051-1056.

Ge, X., Wang, J., Ding, J., Cao, X., Zhang, Z., Liu, J. and Li, X. (2019). Combining UAV-based hyperspectral imagery and machine learning algorithms for soil moisture content monitoring. PeerJ, 7, p.e6926.

Guan, S., Fukami, K., Matsunaka, H., Okami, M., Tanaka, R., Nakano, H., Sakai, T., Nakano, K., Ohdan, H. and Takahashi, K. (2019). Assessing correlation of high-resolution NDVI with fertilizer application level and yield of rice and wheat crops using small UAVs. Remote Sensing, 11(2), p.112.

Hong, Y., Adler, R., and Huffman, G. (2007). "Use of satellite remote sensing data in the mapping of global landslide susceptibility." *Natural Hazards*, 43(2), 245–256.

Klose, M., Highland, L., Damm, B. and Terhorst, B. (2014). Estimation of direct landslide costs in industrialized countries: Challenges, concepts, and case study. Landslide science for a safer geoenvironment, Springer, Cham, 661-667.

Lowe, D.G. (2004). Distinctive image features from scale-invariant keypoints. International journal of computer vision, 60(2), pp.91-110.

Lu, F., Sun, Y. and Hou, F. (2020). Using UAV Visible Images to Estimate the Soil Moisture of Steppe. Water, 12(9), p.2334.

Rossi, G., Tanteri, L., Tofani, V., Vannocci, P., Moretti, S., and Casagli, N. (2018). Multitemporal UAV surveys for landslide mapping and characterization. Landslides, 15(5), 1045-1052.

Ruder, S. (2016). An overview of gradient descent optimization algorithms. arXiv preprint arXiv:1609.04747.

Strecha, C., Bronstein, A., Bronstein, M. and Fua, P. (2011). LDAHash: Improved matching with smaller descriptors. IEEE transactions on pattern analysis and machine intelligence, 34(1), pp.66-78.

Strecha, C., Küng, O. and Fua, P. (2012). Automatic mapping from ultra-light UAV imagery (No. CONF).

Triggs, B., McLauchlan, P.F., Hartley, R.I. and Fitzgibbon, A.W. (1999). Bundle adjustment—a modern synthesis. In International workshop on vision algorithms (pp. 298-372). Springer, Berlin, Heidelberg.

Ugbaje, S., and Bishop, T. (2020). "Hydrological control of vegetation greenness dynamics in Africa: A multivariate analysis using satellite observed soil moisture, terrestrial water storage and precipitation." *Land*, 9(1), 15.

Wicki, A., Lehmann, P., Hauck, C., Seneviratne, S. I., Waldner, P., and Stähli, M. (2020). Assessing the potential of soil moisture measurements for regional landslide early warning. Landslides, 17(8), 1881-1896.

Zanetti, S.S., Cecílio, R.A., Alves, E.G., Silva, V.H. and Sousa, E.F. (2015). Estimation of the moisture content of tropical soils using colour images and artificial neural networks. Catena, 135, pp.100-106.

Zhuo, L., Dai, Q., Han, D., Chen, N., Zhao, B. and Berti, M. (2019). Evaluation of remotely sensed soil moisture for landslide hazard assessment. IEEE Journal of Selected Topics in Applied Earth Observations and Remote Sensing, 12(1), 162-173.